Geophysical Research Letters

RESEARCH LETTER
10.1029/2020GL090951

Nonmonotonic Change of the Arctic Ocean Freshwater Storage Capability in a Warming Climate

Shizhu Wang[1,2,3], Qiang Wang[4], Qi Shu[1,2,3], Zhenya Song[1,2,3], Gerrit Lohmann[4,5,6], Sergey Danilov[4], and Fangli Qiao[1,2,3]

[1]First Institute of Oceanography, and Key Laboratory of Marine Science and Numerical Modeling, Ministry of Natural Resources, Qingdao, China, [2]Laboratory for Regional Oceanography and Numerical Modeling, Pilot National Laboratory for Marine Science and Technology, Qingdao, China, [3]Shandong Key Laboratory of Marine Science and Numerical Modeling, Qingdao, China, [4]Alfred-Wegener-Institut Helmholtz-Zentrum für Polar- und Meeresforschung (AWI), Bremerhaven, Germany, [5]Department of Environmental Physics, University of Bremen, Bremen, Germany, [6]MARUM Center for Marine Environmental Sciences, University of Bremen, Bremen, Germany

Abstract Freshwater in the Arctic Ocean is one of the key climate components. It is not well understood how the capability of the Arctic Ocean to store freshwater will develop when freshwater supplies increase in a warming climate. By using numerical experiments, we find that this capability varies with the Arctic sea ice decline nonmonotonically, with the largest capability at intermediate strength of sea ice decline. Through enhancing the ocean surface stress, sea ice decline not only accumulates freshwater toward the Amerasian Basin but also tends to reduce the amount of freshwater in both the Eurasian and Amerasian basins by increasing the occupation of Atlantic-origin water in the upper ocean. An increase in river runoff modulates the counterbalance of the two competing effects, leading to the nonmonotonic changes of the Arctic freshwater storage capability in a warming climate.

Plain Language Summary The Arctic Ocean is a giant freshwater pool of the Earth System. In a warming climate, the Arctic liquid freshwater content is expected to increase because more freshwater tends to be hosed into the Arctic Ocean. Will the Arctic freshwater storage capability change? In this work, we conducted numerical experiments to show that sea ice is a key controller of the Arctic freshwater storage capability. With the shrinking sea ice, more freshwater is transported from the Eurasian Basin to the Amerasian Basin. In the meanwhile, more saline water fills up the Eurasian Basin and further propagates to the Amerasian Basin too. The opposite effects of these two processes cause a first increasing and then decreasing change in the Arctic freshwater content following the strengthening of the sea ice decline. However, the increase of river runoff can delay the transition between the two phases, leading to a bell-shaped Arctic freshwater storage capability: the maximum capability occurs at moderate strength of sea ice loss. Our study suggests that the impact of sea ice decline should be adequately considered when predicting changes in Arctic Ocean environment and its changing role in the climate.

Key Points:

- Sea ice decline leads to both enhanced freshwater Ekman transport and increased occupation of Atlantic-origin water in the Arctic Ocean
- Counterbalance between the two processes renders a first increasing and then decreasing liquid freshwater content while sea ice declines
- Stronger river runoff modulates the counterbalance and causes nonmonotonic changes of freshwater storage capability in a warming world

Supporting Information:

Supporting Information may be found in the online version of this article.

Correspondence to:

F. Qiao,
qiaofl@fio.org.cn

Citation:

Wang, S., Wang, Q., Shu, Q., Song, Z., Lohmann, G., Danilov, S., & Qiao, F. (2021). Nonmonotonic change of the Arctic Ocean freshwater storage capability in a warming climate. *Geophysical Research Letters*, *48*, e2020GL090951. https://doi.org/10.1029/2020GL090951

Received 23 SEP 2020
Accepted 6 MAY 2021

1. Introduction

Significant increase of liquid freshwater content (FWC) in the Arctic Ocean has been observed since the mid-1990s (Giles et al., 2012; Haine et al., 2015; Proshutinsky et al., 2009, 2019; Rabe et al., 2014). This freshening trend can dramatically impact the biogeochemical processes in the Arctic Ocean (Kipp et al., 2018). A fresher halocline also renders a stronger barrier between the floating sea ice and the warm Atlantic Water at depth (Polyakov et al., 2018; Rudels et al., 1996). If exported to the Atlantic Ocean, the freshwater could significantly impact the large-scale ocean circulation and climate by suppressing deep water formation in the North Atlantic (Condron & Winsor, 2012).

Winds associated with different atmospheric circulation regimes can drive changes in the Arctic freshwater storage (Cornish et al., 2020; Johnson et al., 2018; Manucharyan et al., 2016; Wang, 2021). For example, an anticyclonic wind regime functions to increase Arctic FWC through Ekman convergence and the subsequent downwelling. The response of Arctic FWC to winds, however, can be partially counteracted by eddy fluxes (Davis et al., 2014; Manucharyan & Spall, 2016; Manucharyan et al., 2016; Meneghello et al., 2017), ice-ocean current feedback (Dewey et al., 2018; Meneghello et al., 2018; Wang, Marshall, et al., 2019; Zhong

et al., 2018), and their combined effect (Doddridge et al., 2019; Meneghello et al., 2020; Wang, Marshall, et al., 2019). Furthermore, sea ice is an important mediator of the FWC spatial distribution through its impact on ocean surface stress (Wang, 2021; Wang, Wekerle, et al., 2019).

Freshwater sources for the Arctic Ocean including continental runoff discharge, the Bering Strait inflow, net precipitation minus evaporation, and sea ice meltwater, have been increasing over the past few decades (Carmack et al., 2016; Haine et al., 2015; Woodgate et al., 2018). These changes might be signals of climate change (Jahn & Laiho, 2020), and even stronger increase in Arctic freshwater sources in future warming climate is expected (Shu et al., 2018). With an increase in freshwater supplies, the Arctic FWC will increase even without changes in winds above the Arctic Ocean, although not all excess freshwater will be hold in the Arctic (Brown et al., 2019; Lambert et al., 2019; Nummelin et al., 2016; Weatherly & Walsh, 1996). While these studies documented the response of Arctic FWC to increased freshwater sources, it is still not known whether and to what extent the response is influenced by contemporary changes in the Arctic sea ice state in a warming world.

In this paper, we will test a hypothesis that the increase of Arctic liquid FWC in case of enhanced freshwater supplies can be significantly influenced by the Arctic sea ice state, that is, by sea ice decline induced by the climate change. We will investigate how the freshwater storage capability of the Arctic Ocean will develop in a changing climate. The method and model configuration will be described in Section 2, which is followed by the main results in Section 3. Discussions and conclusions will be given in Sections 4 and 5, respectively.

2. Methods

We employ the global Finite Element Sea ice-Ocean Model (FESOM v1.4, Wang et al., 2014) in this paper. Both its ocean and sea ice components are based on unstructured triangular discretization (Danilov et al., 2004, 2015; Wang et al., 2008). The applied model setup has an intermediate horizontal resolution of 24 km north of about 45°N and a nominal resolution of 1° in most other parts of the global ocean. The eddy diffusivity is scaled with local resolution, and it has a maximum value of 100 m^2/s in the Arctic Ocean as suggested in Wang et al. (2014). The mesh has 47 z-levels with vertical grid spacing of 10 m in the upper 100 m ocean. This mesh has been used in several studies on Arctic freshwater (e.g., Wang et al., 2016; W. Zhang et al., 2020).

The river runoff data of Dai et al. (2009) are used in reference simulations (1*x* runoff). The river freshwater from each river mouth is distributed over 300 km distance from the river mouth to account for unresolved ocean processes in spreading the river water (Wang et al., 2014). The Arctic total river runoff averaged over the simulation period is 0.128 Sv. Arctic river runoff has been increasing in the past few decades (Ahmed et al., 2020) and is expected to increase further in the future (Nummelin et al., 2016; Shu et al., 2018). Thus another two sets of sensitivity simulations are carried out by doubling (2*x* runoff) and tripling (3*x* runoff) the runoff freshwater flux inside the Arctic Ocean (indicated by the red box in the last panel of Figure 1), respectively, for our purpose. Freshwater flux from precipitation minus evaporation is kept unchanged between different simulations.

We use different thermal forcings over the Arctic Ocean to carry out simulations representing different warming scenarios. The historical CORE-II atmospheric forcing fields (Large & Yeager, 2009) are employed to force FESOM all over the globe except the Arctic region. Over the Arctic Ocean, the CORE-II forcing is also used except for the fields related to thermal forcing (i.e., air temperature and downward shortwave and longwave radiation). Specifically, we create six sets of 1-year-long thermal forcing fields with a 6-hourly frequency to represent six different climate states. Two forcing scenarios, Hist7089 and Hist0009, are acquired by averaging the CORE II data in the period of 1970–1989 and 2000–2009, respectively. "Hist" in the names stands for historical forcing. The other four scenarios, named SSP126, SSP245, SSP370, and SSP585, are obtained by averaging the ScenaioMIP (O'Neill et al., 2016) output of AWI-CM (Semmler et al., 2020) over the last 10 years of the 21st century. They correspond to future emission scenarios of SSP1-2.6, SSP2-4.5, SSP3-7.0, and SSP5-8.5, respectively (Figure 1a). Over the Arctic Ocean, the 1-year-long thermal forcing fields are applied repeatedly in each respective simulation. The simulated Arctic sea ice state changes in different runs depending on the Arctic thermal forcing applied (see Section 3, Results).

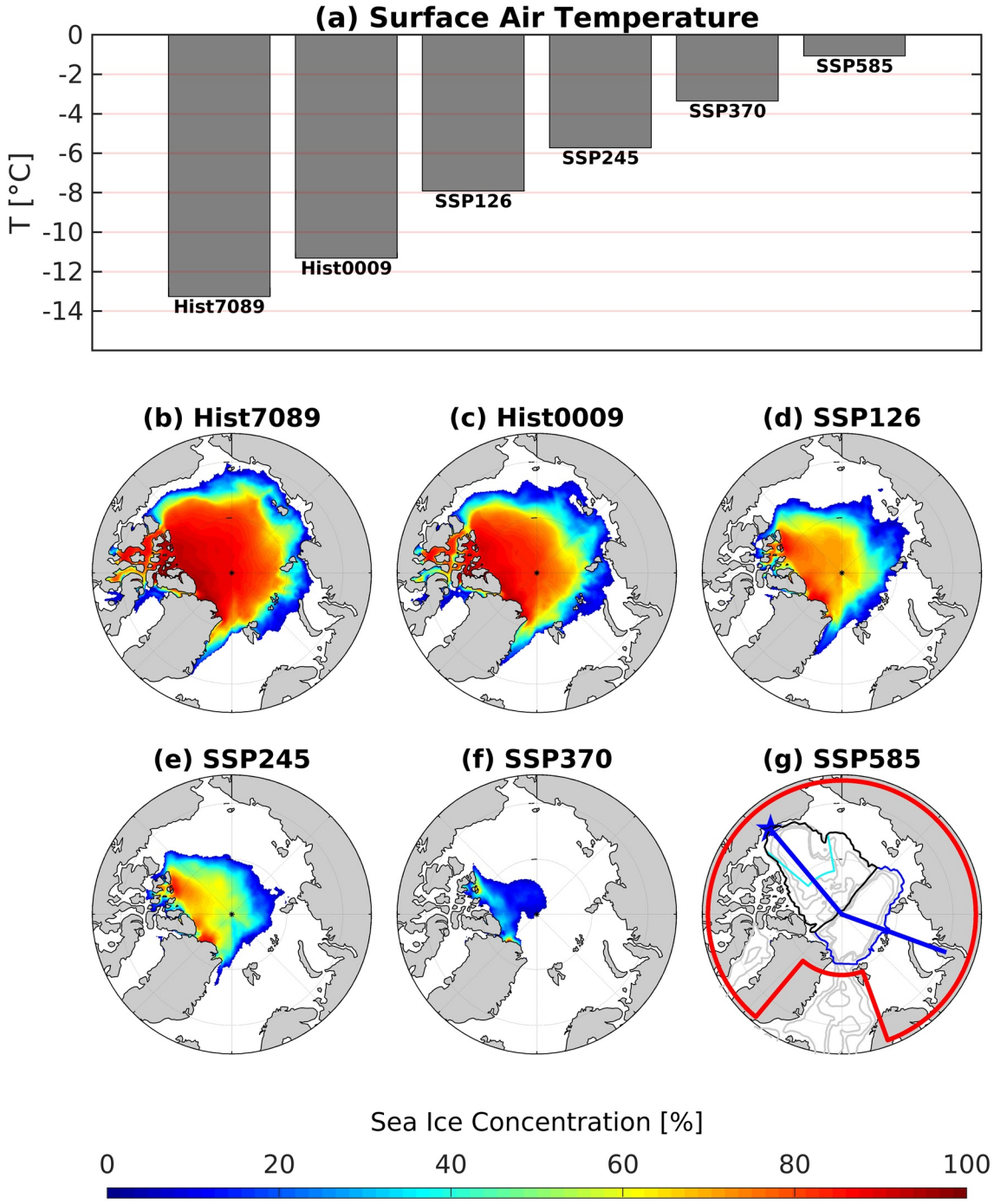

Figure 1. (a) Annual mean surface air temperatures averaged over the Arctic Ocean in the six forcing scenarios. (b–g) Simulated September sea ice concentration under the six forcing scenarios. Sea ice concentration more than 5% is shown. The annual mean sea ice concentration is depicted in Figure S1. September sea ice fully vanishes in SSP585. In panel (g), the red box is where the Arctic thermal forcing is changed, the blue lines marks the section used in Figure 4 and the blue star is the left side of the section. The black and blue boxes denote the Amerasian Basin and the Eurasian Basin, respectively. The Beaufort Gyre region is shown in cyan. The gray contour lines indicate the 500-, 2,000-, and 3,000-m isobaths.

All the simulations start from rest with the initial temperature and salinity fields provided by the annual climatology of PHC3.0 (Steele et al., 2001) and are run for 62 years (1948–2009, one CORE-II forcing loop). In total, we have 18 simulations for three river runoff cases and six Arctic atmospheric thermal forcing states (climate scenarios). Results shown below are the mean of the last 10 years of the simulations. The vertically integrated liquid FWC is defined as

$$\mathrm{FWC} = \int_{D}^{0} \left(S_{\mathrm{ref}} - S\right) / S_{\mathrm{ref}}\, dz$$

where S is ocean salinity, $S_{\mathrm{ref}} = 34.8$ psu is the reference salinity, and D is the isohaline depth of $S = S_{\mathrm{ref}}$. Volumetric FWC is obtained by integrating the vertically integrated FWC laterally.

To better describe the impact of Arctic atmospheric thermal forcing on the response of Arctic liquid FWC to increasing freshwater supplies, we introduce a diagnostic called freshwater storage capability, which is explained in the following. In each climate scenario, the FWC increase due to doubling river runoff relative to the reference case with 1x runoff is given by

$$\Delta\mathrm{FWC}_{2x,\mathrm{scenario}} = \mathrm{FWC}_{2x,\mathrm{scenario}} - \mathrm{FWC}_{1x,\mathrm{scenario}}$$

where $\mathrm{FWC}_{1x,\mathrm{scenario}}$ and $\mathrm{FWC}_{2x,\mathrm{scenario}}$ stand for the FWC in the cases of 1x runoff and 2x runoff forcing, respectively, and scenario in the subscript indicates the employed thermal forcing (one from Hist7089, Hist0009, SSP126, SSP245, SSP370, and SSP585). This calculation is done for each climate scenario separately. For example, in the SSP245 scenario, the FWC increase when runoff is doubled is calculated as

$$\Delta\mathrm{FWC}_{2x,\mathrm{SSP245}} = \mathrm{FWC}_{2x,\mathrm{SSP245}} - \mathrm{FWC}_{1x,\mathrm{SSP245}}.$$

Even with the same increase in river runoff, the changes in Arctic FWC might be different in different climate scenarios. In another word, the ability of the Arctic Ocean to store additional freshwater in response to increasing river runoff might be influenced by Arctic thermal forcing conditions. We are interested to know how this ability will change in different climate scenarios in comparison with the historical scenario of Hist7089. Therefore, we further calculate the ratio between the FWC increase in a certain scenario $\left(\Delta\mathrm{FWC}_{2x,\mathrm{scenario}}\right)$ and the FWC increase in the Hist7089 scenario ($\Delta\mathrm{FWC}_{2x,\mathrm{Hist7089}}$):

$$\mathrm{Capability}_{2x,scenario} = \Delta\mathrm{FWC}_{2x,\mathrm{scenario}} \,/\, \Delta\mathrm{FWC}_{2x,\mathrm{Hist7089}}$$

which is the freshwater storage capability in the considered scenario relative to the Hist7089 scenario. It is calculated for each scenario. If the freshwater storage capability is larger than one in a certain climate scenario, it indicates that the Arctic Ocean in this scenario is able to store more freshwater than in Hist7089 even when river discharge has the same increase. In the particular case for the Hist7089 scenario, $\mathrm{Capability}_{2x,\mathrm{Hist7089}} = 1$ simply because the denominator and numerator are the same in the fraction.

The same analysis is also done for the cases of tripling runoff. Besides calculating the FWC increase and freshwater storage capability for the whole Arctic Ocean, we also do the analysis for the Eurasian Basin (EB) and Amerasian Basin (AB) separately.

3. Results

As expected, the Arctic summer sea ice coverage is lower under warmer thermal forcings (Figure 1). The Arctic Ocean is already close to be sea ice free in summer when forced by the SSP370 scenario. Reduction in sea ice concentration and thickness with increasing climate warming occurs in all seasons, and the simulated annual mean fields in all scenarios are shown in Figures S1 and S2. We note that the Arctic sea ice adjusts to the annually repeated thermal forcing over the Arctic Ocean quickly within the first 10 model years and does not show significant trends afterward. As we are interested in the Arctic FWC at the end of the long simulations, the initial sea ice adjustment does not influence our study. Changes in the simulated sea ice state caused by increasing river runoff are negligible compared to the difference between scenario runs (not shown).

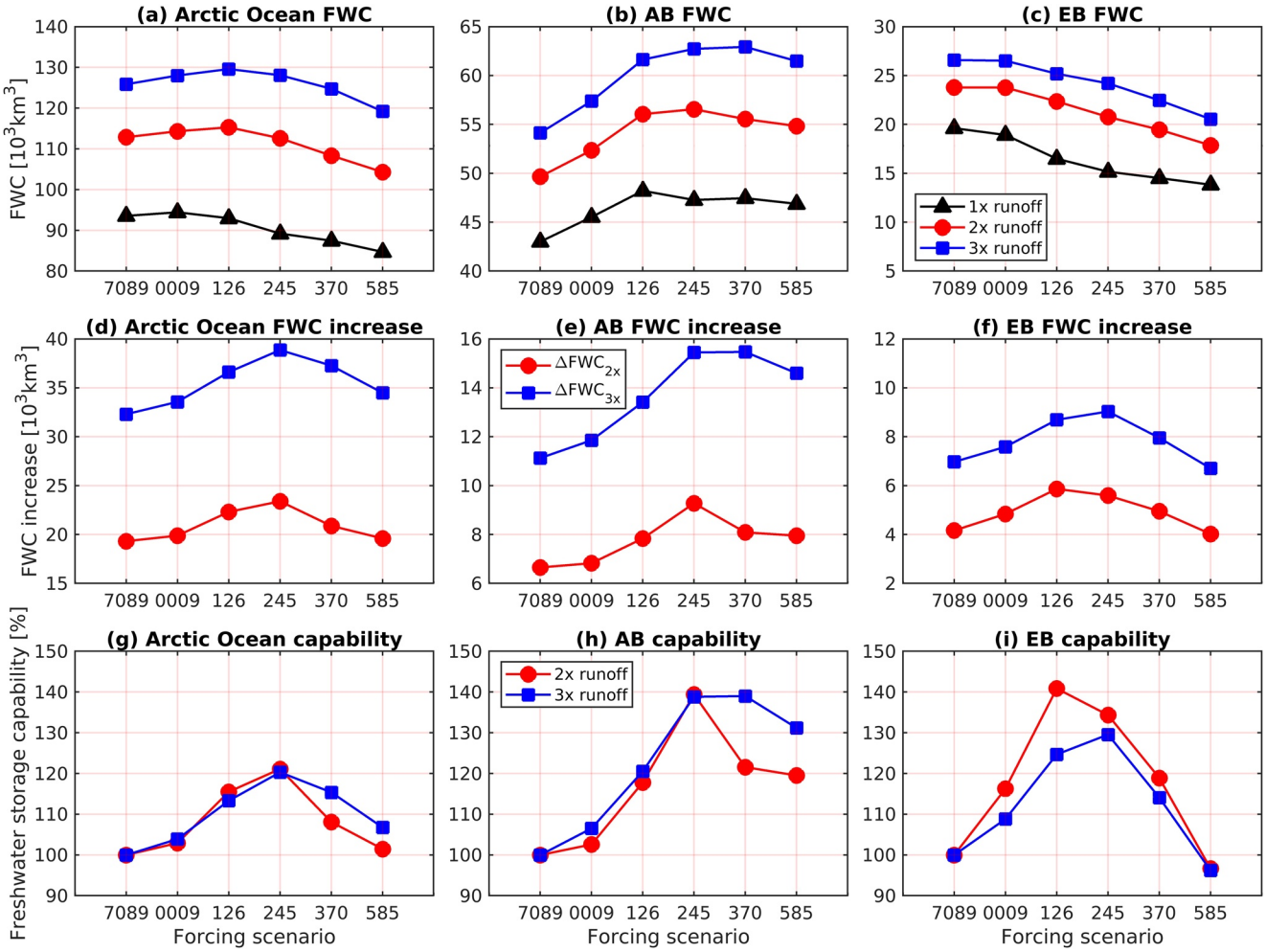

Figure 2. Liquid freshwater content (FWC) in (a) the whole Arctic Ocean, (b) the Amerasian Basin, and (c) the Eurasian Basin. Different colors present different cases of river runoff forcing (see text). (d–f) The FWC increment in the two high river runoff cases referenced to the historical river runoff case in different regions. (g–i) The freshwater storage capability, which is defined as the ratio between the FWC increment in different climate scenarios and that in the Hist7089 scenario.

The changing Arctic thermal forcing exerts important impact on the Arctic FWC: The Arctic FWC increases first and then decreases with the strengthening of atmospheric warming, and this happens in all the three cases of river runoff forcing (Figure 2a). The FWC in the AB also has a maximum at intermediate levels of climate warming (Figure 2b). In the EB, the FWC decreases with increasing warming, although the changes between the first two historical scenarios are relatively small (Figure 2c). It is interesting to note that while the EB FWC is much less than the AB FWC, its change due to atmospheric warming is as significant as that of the AB FWC. Increasing Arctic river runoff results in an increase in Arctic liquid FWC in both the AB and EB for all forcing scenarios.

Atmospheric thermal forcing can affect the FWC spatial distribution (Figure 3). As already revealed by the changes of FWC in Figures 2b and 2c, the amount of freshwater keeps decreasing in the EB with increasing atmospheric warming, while it increases first and then decreases in the AB. The latter decrease occurs because saltier Eurasian water advects to the AB as manifested by the extension of the negative FWC anomaly from the EB toward the Canada basin (Figure 3), which will be further explained below. A similar response of the Arctic FWC spatial distribution to climate scenarios is found in all the three cases of river runoff forcing (Figures S3 and S4).

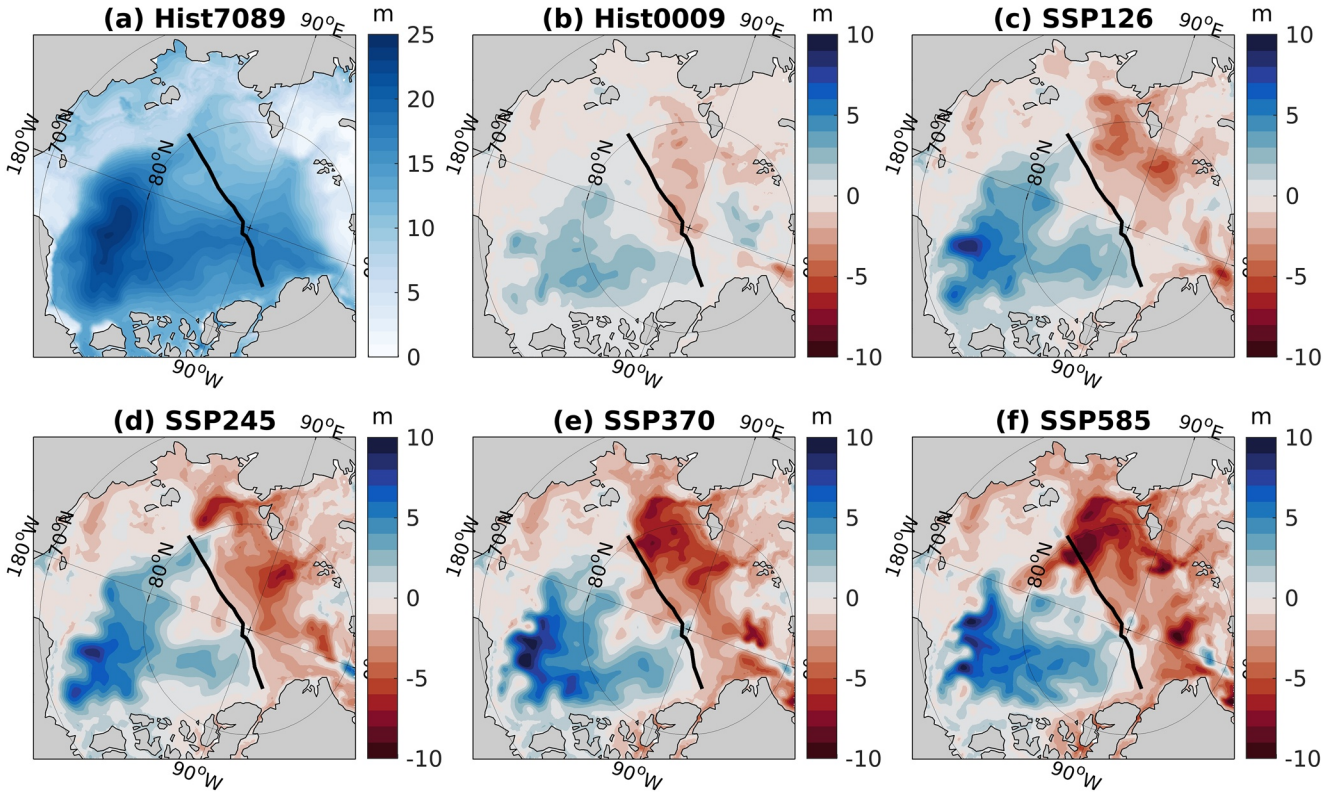

Figure 3. (a) Liquid freshwater content of the Hist7089 scenario and (b–f) the freshwater content anomalies of other scenarios referenced to Hist7089. Liquid freshwater increases in the Amerasian Basin and decreases in the Eurasian Basin when sea ice keeps declining from the coldest to the warmest scenario. With the progress of sea ice decline, the negative anomaly penetrates to the Amerasian Basin too. Only the runs with 1.0 runoff are shown. The results with 2*x* and 3*x* river runoff are shown in the online supplementary Figures S3 and S4. The black curve indicates the Lomonosov Ridge, that is, the boundary of the two deep basins.

The response of the Arctic FWC spatial distribution to atmospheric warming can be explained by the impact of sea ice on ocean surface stress as suggested in previous studies (Wang, 2021; Wang, Wekerle, et al., 2019). Changes in sea ice coverage and internal stress, the latter of which is a function of sea ice concentration and thickness, can significantly influence the ocean surface stress (Martin et al., 2014; Wang, 2021; Wang, Wekerle, et al., 2019). With climate warming, Arctic sea ice declines in thickness and coverage (Figure 1, Figures S1 and S2), which leads to enhanced ocean surface stress (Figures 4a–4c and Figure S5). The changes in ocean surface stress are considered "enhancement" because the stress anomalies are largely along the direction of the climatological ocean surface stress with two major features: anomalies directed from the Eurasian coast to north of the Greenland and anticyclonic anomalies in the Beaufort Gyre region. The corresponding Ekman transport anomalies are directed from the EB to the AB and a convergence toward the Beaufort Gyre (Figures 4d–4f and Figure S6). The strength of the surface stress and Ekman transport exhibits a monotonic change following sea ice reduction. That is, the stronger Arctic sea ice declines, the larger are the ocean surface stress and Ekman transport anomalies (Figures S5 and S6). Changes in atmospheric circulation regimes are able to change the upper ocean circulation and shift the front between Eurasian and Canadian waters (McPhee et al., 2009; Morison et al., 2012; Proshutinsky et al., 2009; Timmermans et al., 2011; Wang, 2021). In our study, the wind forcing remained unchanged among the simulations, so the stress and Ekman transport anomalies are mainly the result of the changes in sea ice.

The ocean salinity changes in response to the surface Ekman transport anomalies described above (Figures 4g–4i and Figure S7). On the one hand, surface freshwater is accumulated toward the Canada Basin; on the other hand, the EB becomes more saline when its freshwater in the upper ocean shifts to the AB, and it is increasingly filled by saline waters of Atlantic origin. In the AB, the freshening happens mainly in the upper 300 m. In the EB, the saline tendency of the upper ocean is associated with a clear uplift of the 34.8 psu

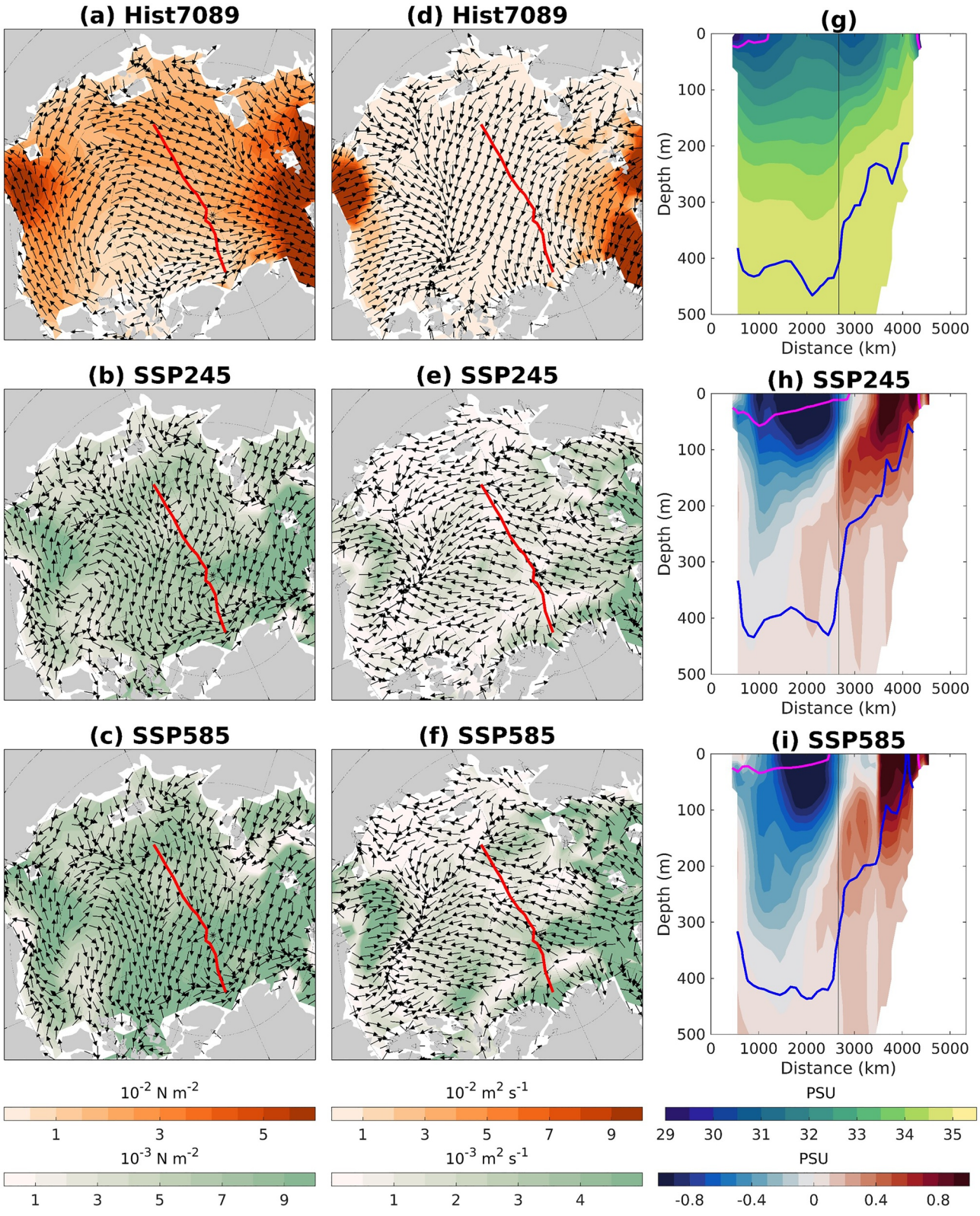
(a) Hist7089
(d) Hist7089
(g)
(b) SSP245
(e) SSP245
(h) SSP245
(c) SSP585
(f) SSP585
(i) SSP585
Depth (m)
Distance (km)
0
100
200
300
400
500
1000
2000
3000
4000
5000
10^{-2} N m^{-2}
1
3
5
10^{-3} N m^{-2}
7
9
10^{-2} m^2 s^{-1}
10^{-3} m^2 s^{-1}
2
4
PSU
29
30
31
32
33
34
35
-0.8
-0.4
0
0.4
0.8

isohaline. Due to limited amount of surface freshwater to supply from the EB to the AB, saline anomalies can even extend into the AB with enhanced sea ice decline (Figures 4g–4i and Figure S7). This explains why the liquid FWC in the AB increases first and then decreases when sea ice continues to decline (Figure 2b). The signal of persistent saline tendency in the EB also propagates to the AB at depth as a result of cyclonic ocean circulation, as manifested by the weakly positive salinity anomaly at depth in the AB with increasing atmospheric warming (Figures 4g–4i and Figure S7). This can also contribute to the AB FWC decrease in the strong warming scenarios, but the upward trend of AB FWC in the relatively weak warming scenarios is due to the upper ocean changes.

Comparing Hist7089 and Hist0009 in the historical river runoff case indicates that the total Arctic liquid FWC is not significantly impacted by the past sea ice decline (black curve in Figure 2a). However, sea ice decline does increase the accumulation of freshwater in the AB and reduce it in the EB (Figures 2b and 2c) through changing the ocean surface stress (Figure 4). The FWC over the continental shelf is also slightly reduced (not shown). The opposite changes largely compensate, resulting in a very small change in the total FWC between the two scenarios (Figure 2a). This is consistent with the finding by Wang, Wekerle, et al. (2019) who studied the impact of sea ice decline on Arctic FWC over the past few decades. Our simulations show that the Arctic total liquid FWC will keep decreasing if sea ice continues to shrink in future warming scenarios (black curve in Figure 2a). However, if river runoff is doubled or tripled, the total liquid FWC will increase until the SSP126 scenario and then drop in stronger warming scenarios (red and blue curves in Figure 2a). The delayed emergence of decreasing trends in Arctic total FWC in cases of higher runoff is because the enlarged freshwater supply delays the emergence of decreasing trends in the AB (Figure 2b) and reduces the decreasing trends in the EB as well (Figure 2c). However, a stronger river runoff can weaken, but cannot prevent, the salinification effect of the enhanced ocean surface stress associated with sea ice decline.

After understanding the dynamical processes through which sea ice decline influences the Arctic upper ocean salinity and liquid FWC, we can answer our main question: if the freshwater supply increases in the future warming climate, which is very likely to occur (Shu et al., 2018), will the response of the Arctic liquid FWC be influenced by the state of Arctic sea ice? To answer this question, we calculate the FWC increase (see Section 2, Methods) for all the scenarios (Figures 2d–2f). The FWC increases caused by stronger river runoff are different among different climate scenarios for both the Arctic basins and the whole Arctic Ocean. Interestingly, they have maxima in intermediate warming scenarios. The reason for this behavior is mentioned above: larger river runoff delays the emergence of the decreasing trend in FWC in the AB and reduces the decreasing trend in the EB until intermediate warming scenarios (Figures 2a–2c). As a result, the difference of FWC between cases of different river runoff forcing has (quasi) bell-shapes (Figures 2d–2f).

The freshwater storage capability (see the definition in Methods) is calculated for the whole Arctic Ocean and the two deep basins separately (Figures 2g–2i). It has bell-shapes with maxima of about 140% in the AB and 130%–140% in the EB. In both basins, the maxima in the case of stronger river runoff forcing are located at stronger warming scenarios. Integrated over the whole Arctic Ocean, the maximal freshwater storage capability is still as high as 120% with both river runoff forcings. This value is lower than those in both the AB and EB because the FWC increase over the continental shelf is large and does not differ much in different climate scenarios (that is, a larger denominator when calculating the ratio).

In summary, our above diagnostic of the freshwater storage capability reveals that future Arctic atmospheric warming can significantly enhance the storage of freshwater under the forcing of increased freshwater supplies: by up to 40% in the Arctic main basins and by 20% for the whole Arctic Ocean. However, these maximal storage capabilities are not in the scenarios with the strongest atmospheric warming.

Figure 4. The top row shows (a) the ocean surface stress, (d) the Ekman transport and (g) the vertical salinity transect of the Hist7089 simulation. Anomalies of (b and c) ocean surface stress, (e and f) Ekman transport, and (h–i) salinity in SSP245 and SSP585 referenced to Hist7089 are shown in the middle and the bottom rows, respectively. Arrow shows the direction and shading shows the amplitude. In the bottom of each column, the two color bars correspond to the value in the Hist7089 scenario (upper panel) and anomalies relative to Hist7089 (middle and bottom panels). The purple and blue lines in the right panels are the 30.5 and 34.8 psu isohalines of the corresponding experiment, respectively. The vertical black lines indicate the North Pole. The location of the section in the right panels is marked by the blue lines in Figure 1g. The red curve indicates the Lomonosov Ridge, that is, the boundary of the two deep basins. The three anomaly fields for all the studied climate scenarios are shown in the online supplementary Figures S5–S7.

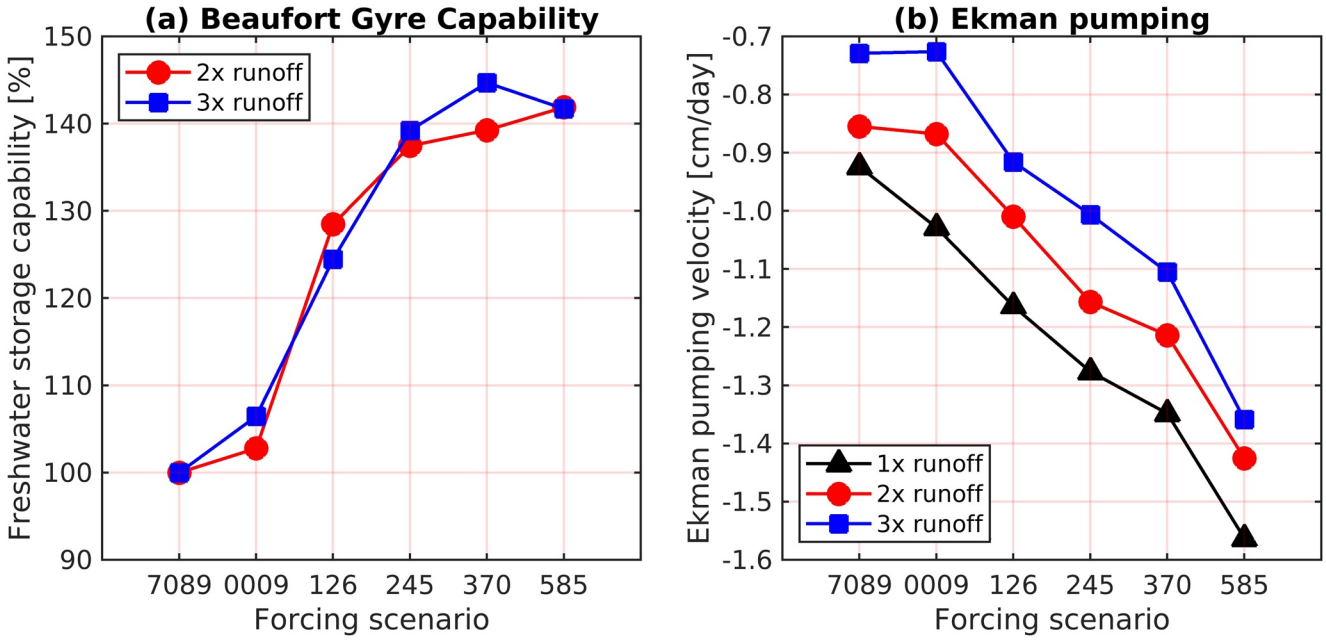

Figure 5. (a) Freshwater storage capability and (b) the Ekman pumping velocity in the Beaufort Gyre.

4. Discussions

As the largest freshwater reservoir in the Arctic Ocean, the BG is on average an Ekman downwelling region (Proshutinsky et al., 2009). Observation has shown a significant increase of more than 6,400 km^3 in the BG FWC from 2003 to 2018 (Proshutinsky et al., 2019), which is attributed to the persistent anticyclonic atmospheric wind regime accompanied by sea ice decline (Wang et al., 2018). In our simulations with historical river runoff, each run can reasonably reproduce the BG FWC peaking after 2000 (Figure S8), although changes in sea ice can affect the ocean surface stress and thus the amount of freshwater accumulated therein. With the atmospheric warming, the BG freshwater storage capability will also increase by about 40% (Figure 5a). Within the studied warming scenarios, the curve of the freshwater storage capability for the BG does not have a bell-shape as for the AB and EB (Figures 2g–2i) because the BG is impacted by the Atlantic water later than other regions due to its geographic location. However, the impact has become obvious starting from the SSP370 scenario as shown by the leveling-off of the curve (Figure 5a).

Availability of freshwater for accumulation is a key factor determining the BG FWC (Proshutinsky et al., 2019; Wang et al., 2018). Our findings further support this argument. The Ekman downwelling in the AB, including the BG region (Figure 5b), strengthens with sea ice decline. However, because the availability of freshwater decreases due to salinification originating from the EB (Figure 3), the FWC in the AB and BG does not increase monotonically as the tendency of Ekman downwelling suggests. Furthermore, the Ekman downwelling in the BG becomes weaker with increasing river runoff in all forcing scenarios. This is a nice evidence for the existence of ocean-ice current feedback on the ocean-ice stress and FWC (Dewey et al., 2018; Meneghello et al., 2018; Wang, Marshall, et al., 2019; Zhong et al., 2018). Larger river runoff increases the FWC, thus the ocean surface current, which then reduces the ocean surface stress and Ekman downwelling. The latter constrains the accumulation of freshwater. However, the availability of freshwater plays the leading role in determining the FWC tendency, as the FWC increases with the increase of river runoff and the negative feedback comes into play following the increase of the FWC.

The rising runoff can increase the amount of freshwater exiting the Arctic Ocean, leading to negative surface salinity anomaly and thus suppressing deep-water formation in the Labrador and Nordic seas (see the mixed layer distribution in Figure S9). In future warming climate, however, deep convection might occur in the Arctic Ocean when the seasonal sea ice edge migrates northwards (Lique et al., 2018). We find that sea ice decline can lead to the salinification of the upper ocean, which is the strongest in the EB and may occur

even when Arctic freshwater supply is enhanced. This effect of sea ice decline could be an important driver for weakening Arctic Ocean stratification and preconditioning deep convection.

Eddy transport counteracts the accumulation of freshwater by Ekman convergence (Manucharyan & Spall, 2016; Meneghello et al., 2017). The recent study by Spall (2020) indicates that the exchange between the two deep basins is not only influenced by main flows, but also by eddy fluxes. In this study, the model resolution is not eddy resolving and eddies are parameterized, as in most numerical studies on the dynamics of the Arctic freshwater (e.g., Cornish et al., 2020; Jahn & Laiho, 2020; Lique et al., 2018; Wang, Marshall, et al., 2019; J. Zhang et al., 2016). Parameterizations might cause uncertainty in the quantitative results. For example, if higher eddy diffusivity were chosen in our simulations, the sensitivity of FWC to sea ice changes might become weaker because freshwater release would be larger. Nevertheless, we believe our qualitative findings are plausible with respect to the dynamical processes investigated. It is expected that eddy-resolving models with kilometer resolution, which just start to emerge (Wang et al., 2020), will further improve our skills in understanding and predicting the Arctic Ocean dynamics in the future.

In the simulations, the enforced atmospheric warming not only causes sea ice decline but also warms the ocean through both increased atmospheric heat source and reduced sea ice coverage. Our analysis of dynamic linkages between ocean salinity changes and the anomalies of surface Ekman transport suggests that the changes in ocean surface stress associated with sea ice decline play a crucial role in determining the identified behavior of Arctic freshwater storage. Therefore, we argued that the nonmonotonic changes of Arctic FWC with increasing atmospheric warming in Figures 2a–2c are mainly due to sea ice decline. This argument is supported by the findings of detailed analysis of water masses in simulations with prescribed atmospheric warming in the previous study by Wang, Wekerle, et al. (2019). They have the same conclusion that changes in surface stress and Ekman transport associated with sea ice decline in a warming climate strongly influence the spatial distribution of different water masses and the FWC. Our analysis does not exclude possible impact of ocean circulation changes due to Arctic Ocean warming. Strictly speaking, the nonmonotonic changes of Arctic FWC are due to atmospheric warming prescribed. But sea ice decline is arguably the most important impact pathway through which atmospheric warming induces the nonmonotonic changes of Arctic FWC.

We found that freshwater transports through Arctic gateways can also be influenced by Arctic surface thermal forcing. In our particular simulations, the freshwater inflow through the Bering Strait slightly increases with Arctic atmospheric warming monotonically, while the total Arctic freshwater export (sum over all Arctic gateways) increases first and then decreases with atmospheric warming (Figure S10). These changes cannot explain the nonmonotonic change of FWC with largest values in intermediate warming scenarios (Figures 2a and 2b). This further addresses that the changes in the occupation of Atlantic derived water in replacement of freshwater in the upper Arctic Ocean (Figures 4g–4i and Figure S7) plays an important role in determining changes in Arctic FWC. The dynamic responses of freshwater transports through different Arctic gateways to climate change need to be further investigated in future work.

5. Conclusions

Freshwater supplies to the Arctic Ocean are expected to increase in the future. Using dedicated numerical simulations, we proved our hypothesis that the freshwater storage in the Arctic Ocean in response to the increase in Arctic river runoff can be significantly influenced by Arctic atmospheric thermal forcing, in particular by sea ice decline. The freshwater storage capability, a measure of the ability to increase FWC in case freshwater supplies are enhanced, will increase first and then decrease in both Arctic deep basins when sea ice continues to decline in a warming world, even though ocean surface stress and Ekman transport increase monotonically. The maximum capability will occur with intermediate strength of sea ice decline. Our simulations show that the maximum freshwater storage capability in the Arctic deep basins, including Eurasian Basin (EB), Amerasian Basin (AB), and Beaufort Gyre, can increase by about 40% compared to the historical period (1970–1989).

Our study indicates that sea ice is an important controller of the Arctic freshwater storage capability and upper ocean salinity. Sea ice decline enhances ocean surface stress and Ekman transport. On the one hand, more freshwater is transported from the EB to the AB, tending to increase FWC in the AB. On the other

hand, high-salinity water of Atlantic origin fills up the EB and even further spreads toward the AB, resulting in a FWC decrease. As a result, with persistent sea ice decline, the FWC increases and then decreases in the AB, and tends to decrease in the EB. However, increasing river runoff modulates the counterbalance between the two competing processes. An increase in river runoff delays the emergence of the decreasing trend in FWC in the AB and reduces the decreasing trend in the EB until intermediate warming scenarios. Consequently, the difference of FWC between cases of different river runoff forcing first increases and then decreases with sea ice decline, leading to a bell shape in the freshwater storage capability. Predicting future changes in Arctic hydrography in the upper ocean and freshwater storage demands the impacts of sea ice decline and saline Atlantic Water to be adequately considered.

Our study further suggests that the upper ocean stratification, especially in the EB and central Arctic, can be significantly weakened by sea ice decline, which can precondition winter deep convection. The possibility and timing of the deep-convection occurrence depend on the competing effects of sea ice decline and increases in Arctic freshwater supplies. The experiment setup in our study, employing a forced ocean-ice model rather than a coupled climate model, enables us to reveal and quantify the effect of important dynamical processes while excluding complex climate feedbacks. In order to better understand and predict the role of Arctic Ocean in global climate, all the related processes, including what we investigated in this paper and possible climate feedbacks that we neglected, need to be faithfully simulated in climate models.

Conflict of Interest

The authors declare no conflicts of interest relevant to this study.

Data Availability Statement

Data supporting this study are available from http://data.fio.org.cn/qiaofl/WSZ-GRL-2020/fesom_freshwater.zip.

Acknowledgments
This research was jointly supported by the National Natural Science Foundation of China (Grant No. 41821004, F. Qiao), the Helmholtz Climate Initiative REKLIM (Regional Climate Change, Q. Wang), and the Collaborative Research Centre TRR 181 "Energy Transfer in Atmosphere and Ocean" funded by the Deutsche Forschungsgemeinschaft (DFG, German Research Foundation) with Project number 274762653 (S. Danilov). Q. Shu was supported by the Chinese Natural Science Foundation (41941012) and the Basic Scientific Fund for National Public Research Institute of China (ShuXingbei Young Talent Program 2019S06). We thank Gianluca Meneghello and two anonymous reviewers for their helpful comments and suggestions.

References

Ahmed, R., Prowse, T., Dibike, Y., Bonsal, B., & O'Neil, H. (2020). Recent trends in freshwater influx to the arctic ocean from four major arctic-draining rivers. *Water*, *12*(4), 1189. https://doi.org/10.3390/w12041189

Brown, N. J., Nilsson, J., & Pemberton, P. (2019). Arctic ocean freshwater dynamics: Transient response to increasing river runoff and precipitation. *Journal of Geophysical Research: Oceans*, *124*, 5205–5219. https://doi.org/10.1029/2018jc014923

Carmack, E. C., Yamamoto-Kawai, M., Haine, T. W. N., Bacon, S., Bluhm, B. A., Lique, C., et al. (2016). Freshwater and its role in the Arctic Marine System: Sources, disposition, storage, export, and physical and biogeochemical consequences in the Arctic and global oceans. *Journal of Geophysical Research: Biogeosciences*, *121*(3), 675–717. https://doi.org/10.1002/2015JG003140

Condron, A., & Winsor, P. (2012). Meltwater routing and the Younger Dryas. *Proceedings of the National Academy of Sciences of the United States of America*, *109*(49), 19928–19933. https://doi.org/10.1073/pnas.1207381109

Cornish, S. B., Kostov, Y., Johnson, H. L., & Lique, C. (2020). Response of Arctic freshwater to the Arctic oscillation in coupled climate models. *Journal of Climate*, *33*(2020), 2533–2555. https://doi.org/10.1175/jcli-d-19-0685.1

Dai, A., Qian, T., Trenberth, K. E., & Milliman, J. D. (2009). Changes in continental freshwater discharge from 1948 to 2004. *Journal of Climate*, *22*(10), 2773–2792. https://doi.org/10.1175/2008jcli2592.1

Danilov, S., Kivman, G., & Schröter, J. (2004). A finite-element ocean model: Principles and evaluation. *Ocean Modelling*, *6*(2), 125–150. https://doi.org/10.1016/s1463-5003(02)00063-x

Danilov, S., Wang, Q., Timmermann, R., Iakovlev, N., Sidorenko, D., Kimmritz, M., et al. (2015). Finite-Element Sea Ice Model (FESIM), version 2. *Geoscientific Model Development*, *8*, 1747–1761. https://doi.org/10.5194/gmd-8-1747-2015

Davis, P. E. D., Lique, C., & Johnson, H. L. (2014). On the link between Arctic sea ice decline and the freshwater content of the Beaufort Gyre: Insights from a simple process model. *Journal of Climate*, *27*(21), 8170–8184. https://doi.org/10.1175/jcli-d-14-00090.1

Dewey, S., Morison, J., Kwok, R., Dickinson, S., Morison, D., & Andersen, R. (2018). Arctic ice-ocean coupling and gyre equilibration observed with remote sensing. *Geophysical Research Letters*, *45*(3), 1499–1508. https://doi.org/10.1002/2017gl076229

Doddridge, E. W., Meneghello, G., Marshall, J., Scott, J., & Lique, C. (2019). A three-way balance in the Beaufort Gyre: The ice-ocean governor, wind stress, and eddy diffusivity. *Journal of Geophysical Research: Oceans*, *124*(5), 3107–3124. https://doi.org/10.1029/2018jc014897

Giles, K. A., Laxon, S. W., Ridout, A. L., Wingham, D. J., & Bacon, S. (2012). Western Arctic Ocean freshwater storage increased by wind-driven spin-up of the Beaufort Gyre. *Nature Geoscience*, *5*(3), 194–197. https://doi.org/10.1038/ngeo1379

Haine, T. W. N., Curry, B., Gerdes, R., Hansen, E., Karcher, M., Lee, C., et al. (2015). Arctic freshwater export: Status, mechanisms, and prospects. *Global and Planetary Change*, *125*, 13–35. https://doi.org/10.1016/j.gloplacha.2014.11.013

Jahn, A., & Laiho, R. (2020). Forced changes in the Arctic freshwater budget emerge in the early 21st century. *Geophysical Research Letters*, *47*(15), e2020GL088854.

Johnson, H. L., Cornish, S. B., Kostov, Y., Beer, E., & Lique, C. (2018). Arctic Ocean freshwater content and its decadal memory of sea-level pressure. *Geophysical Research Letters*, *45*(10), 4991–5001. https://doi.org/10.1029/2017GL076870

Kipp, L. E., Charette, M. A., Moore, W. S., Henderson, P. B., & Rigor, I. G. (2018). Increased fluxes of shelf-derived materials to the central Arctic Ocean. *Science Advances*, *4*(1), eaao1302. https://doi.org/10.1126/sciadv.aao1302

Lambert, E., Nummelin, A., Pemberton, P., & Ilıcak, M. (2019). Tracing the imprint of river runoff variability on Arctic water mass transformation. *Journal of Geophysical Research: Oceans*, *124*(1), 302–319. https://doi.org/10.1029/2017JC013704
Large, W. G., & Yeager, S. G. (2009). The global climatology of an interannually varying air-sea flux data set. *Climate Dynamics*, *33*(2–3), 341–364. https://doi.org/10.1007/s00382-008-0441-3
Lique, C., Johnson, H. L., & Plancherel, Y. (2018). Emergence of deep convection in the Arctic Ocean under a warming climate. *Climate Dynamics*, *50*(9–10), 3833–3847. https://doi.org/10.1007/s00382-017-3849-9
Manucharyan, G. E., & Spall, M. A. (2016). Wind-driven freshwater buildup and release in the Beaufort Gyre constrained by mesoscale eddies. *Geophysical Research Letters*, *43*(1), 273–282. https://doi.org/10.1002/2015gl065957
Manucharyan, G. E., Spall, M. A., & Thompson, A. F. (2016). A theory of the wind-driven beaufort gyre variability. *Journal of Physical Oceanography*, *46*(11), 3263–3278. https://doi.org/10.1175/JPO-D-16-0091.1
Martin, T., Steele, M., & Zhang, J. (2014). Seasonality and long-term trend of Arctic Ocean surface stress in a model. *Journal of Geophysical Research: Oceans*, *119*(3), 1723–1738. https://doi.org/10.1002/2013jc009425
McPhee, M. G., Proshutinsky, A., Morison, J. H., Steele, M., & Alkire, M. B. (2009). Rapid change in freshwater content of the Arctic Ocean. *Geophysical Research Letters*, *36*(10). https://doi.org/10.1029/2009gl037525
Meneghello, G., Doddridge, E., Marshall, J., Scott, J., & Campin, J.-M. (2020). Exploring the role of the "ice-ocean governor" and mesoscale eddies in the equilibration of the Beaufort Gyre: Lessons from observations. *Journal of Physical Oceanography*, *50*(1), 269–277. https://doi.org/10.1175/jpo-d-18-0223.1
Meneghello, G., Marshall, J., Campin, J. M., Doddridge, E., & Timmermans, M. L. (2018). The ice-ocean governor: Ice-ocean stress feedback limits Beaufort Gyre spin-up. *Geophysical Research Letters*, *45*(20), 11293–11299. https://doi.org/10.1029/2018GL080171
Meneghello, G., Marshall, J., Cole, S. T., & Timmermans, M. (2017). Observational inferences of lateral eddy diffusivity in the halocline of the Beaufort Gyre. *Geophysical Research Letters*, *44*(24), 12–331. https://doi.org/10.1002/2017gl075126
Morison, J., Kwok, R., Peralta-Ferriz, C., Alkire, M., Rigor, I., Andersen, R., & Steele, M. (2012). Changing Arctic Ocean freshwater pathways. *Nature*, *481*(7379), 66–70. https://doi.org/10.1038/nature10705
Nummelin, A., Ilicak, M., Li, C., & Smedsrud, L. H. (2016). Consequences of future increased Arctic runoff on Arctic Ocean stratification, circulation, and sea ice cover. *Journal of Geophysical Research: Oceans*, *121*(1), 617–637. https://doi.org/10.1002/2015jc011156
O'Neill, B. C., Tebaldi, C., Van Vuuren, D. P., Eyring, V., Friedlingstein, P., Hurtt, G., et al. (2016). The scenario model intercomparison project (ScenarioMIP) for CMIP6. *Geoscientific Model Development*, *9*, 3461–3482. https://doi.org/10.5194/gmd-9-3461-2016
Polyakov, I. V., Pnyushkov, A. V., & Carmack, E. C. (2018). Stability of the arctic halocline: A new indicator of arctic climate change. *Environmental Research Letters*, *13*(12), 125008. https://doi.org/10.1088/1748-9326/aaec1e
Proshutinsky, A., Krishfield, R., Timmermans, M.-L., Toole, J., Carmack, E., McLaughlin, F., et al. (2009). Beaufort Gyre freshwater reservoir: State and variability from observations. *Journal of Geophysical Research*, *114*(C1). https://doi.org/10.1029/2008jc005104
Proshutinsky, A., Krishfield, R., Toole, J., Timmermans, M., Williams, W., Zimmerman, S., et al. (2019). Analysis of the Beaufort Gyre freshwater content in 2003-2018. *Journal of Geophysical Research: Oceans*, *124*(12), 9658–9689.
Rabe, B., Karcher, M., Kauker, F., Schauer, U., Toole, J. M., Krishfield, R. A., et al. (2014). Arctic Ocean basin liquid freshwater storage trend 1992-2012. *Geophysical Research Letters*, *41*(3), 961–968. https://doi.org/10.1002/2013gl058121
Rudels, B., Anderson, L. G., & Jones, E. P. (1996). Formation and evolution of the surface mixed layer and halocline of the Arctic Ocean. *Journal of Geophysical Research*, *101*(C4), 8807–8821. https://doi.org/10.1029/96jc00143
Semmler, T., Pithan, F., & Jung, T. (2020). Quantifying two-way influences between the Arctic and mid-latitudes through regionally increased CO2 concentrations in coupled climate simulations. *Climate Dynamics*, 1–15.
Shu, Q., Qiao, F., Song, Z., Zhao, J., & Li, X. (2018). Projected Freshening of the Arctic Ocean in the 21st Century. *Journal of Geophysical Research: Oceans*, *123*(12), 9232–9244. https://doi.org/10.1029/2018JC014036
Spall, M. (2020). Potential vorticity dynamics of the Arctic Halocline. *Journal of Physical Oceanography*, *50*(9), 2491–2506. https://doi.org/10.1175/jpo-d-20-0056.1
Steele, M., Morley, R., & Ermold, W. (2001). PHC: A global ocean hydrography with a high-quality Arctic Ocean. *Journal of Climate*, *14*(9), 2079–2087. https://doi.org/10.1175/1520-0442(2001)014<2079:pagohw>2.0.co;2
Timmermans, M., Proshutinsky, A., Krishfield, R. A., Perovich, D. K., Richter-Menge, J. A., Stanton, T. P., & Toole, J. M. (2011). Surface freshening in the Arctic Ocean's Eurasian Basin: An apparent consequence of recent change in the wind-driven circulation. *Journal of Geophysical Research*, *116*(C8). https://doi.org/10.1029/2011jc006975
Wang, Q. (2021). Stronger variability in the Arctic Ocean induced by sea ice decline in a warming climate: Freshwater storage, dynamic sea level and surface circulation. *Journal of Geophysical Research: Oceans*, *126*, 1–19. https://doi.org/10.1029/2020jc016886
Wang, Q., Danilov, S., & Schröter, J. (2008). Finite element ocean circulation model based on triangular prismatic elements, with application in studying the effect of topography representation. *Journal of Geophysical Research*, *113*(C5). https://doi.org/10.1029/2007jc004482
Wang, Q., Danilov, S., Sidorenko, D., Timmermann, R., Wekerle, C., Wang, X., et al. (2014). The Finite Element Sea Ice-Ocean Model (FESOM) v.1.4: Formulation of an ocean general circulation model. *Geoscientific Model Development*, *7*(2), 663–693. https://doi.org/10.5194/gmd-7-663-2014
Wang, Q., Ilicak, M., Gerdes, R., Drange, H., Aksenov, Y., Bailey, D. A., et al. (2016). An assessment of the Arctic Ocean in a suite of interannual CORE-II simulations. Part II: Liquid freshwater. *Ocean Modelling*, *99*, 86–109. https://doi.org/10.1016/j.ocemod.2015.12.009
Wang, Q., Koldunov, N. V., Danilov, S., Sidorenko, D., Wekerle, C., Scholz, P., et al. (2020). Eddy kinetic energy in the Arctic Ocean from a global simulation with a 1-km Arctic. *Geophysical Research Letters*, *47*(14), e2020GL088550. https://doi.org/10.1029/2020gl088550
Wang, Q., Marshall, J., Scott, J., Meneghello, G., Danilov, S., & Jung, T. (2019). On the feedback of ice-ocean stress coupling from geostrophic currents in an anticyclonic wind regime over the Beaufort Gyre. *Journal of Physical Oceanography*, *49*(2), 369–383. https://doi.org/10.1175/jpo-d-18-0185.1
Wang, Q., Wekerle, C., Danilov, S., Koldunov, N., Sidorenko, D., Sein, D., et al. (2018). Arctic Sea ice decline significantly contributed to the unprecedented liquid freshwater accumulation in the Beaufort Gyre of the Arctic Ocean. *Geophysical Research Letters*, *45*(10), 4956–4964. https://doi.org/10.1029/2018GL077901
Wang, Q., Wekerle, C., Danilov, S., Sidorenko, D., Koldunov, N., Sein, D., et al. (2019). Recent sea ice decline did not significantly increase the total liquid freshwater content of the Arctic Ocean. *Journal of Climate*, *32*(1), 15–32. https://doi.org/10.1175/JCLI-D-18-0237.1
Weatherly, J. W., & Walsh, J. E. (1996). The effects of precipitation and river runoff in a coupled ice-ocean model of the Arctic. *Climate Dynamics*, *12*(11), 785–798. https://doi.org/10.1007/s003820050143
Woodgate, R. A. (2018). Increases in the Pacific inflow to the Arctic from 1990 to 2015, and insights into seasonal trends and driving mechanisms from year-round Bering Strait mooring data. *Progress in Oceanography*, *160*, 124–154. https://doi.org/10.1016/j.pocean.2017.12.007

Zhang, J., Steele, M., Runciman, K., Dewey, S., Morison, J., Lee, C., et al. (2016). The Beaufort Gyre intensification and stabilization: A model-observation synthesis. *Journal of Geophysical Research: Oceans*, *121*(11), 7933–7952. https://doi.org/10.1002/2016JC012196

Zhang, W., Wang, Q., Wang, X., & Danilov, S. (2020). Mechanisms driving the interannual variability of the Bering Strait throughflow. *Journal of Geophysical Research: Oceans*, *125*(2), e2019JC015308. https://doi.org/10.1029/2019jc015308

Zhong, W., Steele, M., Zhang, J., & Zhao, J. (2018). Greater role of geostrophic currents in Ekman dynamics in the Western Arctic Ocean as a mechanism for Beaufort Gyre stabilization. *Journal of Geophysical Research: Oceans*, *123*(1), 149–165. https://doi.org/10.1002/2017JC013282